was digested with Eco RI, fractionated on 0.7% agarose, blotted onto Hybond-N (Amersham), and hybridized as described [J. Sambrook, A. Frisch, T. Maniatis, *Molecular Cloning: A Laboratory Manual* (Cold Spring Harbor Laboratory, Cold Spring Harbor, NY, 1989)].
16. Protoplasts from *N. tabacum* SR1 [P. Maliga, A. S.-Breznovits, L. Marton, F. Joo, *Nature* **255**, 401 (1975)] were isolated [J. Draper, R. Scott, P. Armitage, R. Walden, *Plant Genetic Transformation and Gene Expression: A Laboratory Manual* (Blackwell, Oxford, 1988)] and cocultivated with *Agrobacterium* that contained pPCVICEn4HPT as described [A. Depicker *et al.*, *Mol. Gen. Genet.* **201**, 477 (1985)]. Protoplasts were cultured in the presence of hygromycin (15 μg/ml) (Boehringer Mannheim) and Claforan (500 μg/ml) (Hoechst, Frankfurt, Germany) with either cytokinin (kinetin, 0.2 mg/l) (Sigma) and auxin (1-naphthaleneacetic acid, NAA, 1.0 mg/l) (Sigma) or the same media lacking auxin. Calli growing in the absence of auxin were cultured further to form plants.
17. I. Negrutiu *et al.*, *Plant Mol. Biol.* **8**, 363 (1987).
18. We thank the members of our laboratory for their support, especially C. Fromental for protoplast transformations, K. Fritze for callus maintenance, and P. Ljungcrantz for help and discussions, as well as S. Rechmann for help with the DNA sequencing. Special thanks to C. Koncz, D. Wegener, R. Wingender, and E. Buschfeld for advice, discussion, clones, and comments on the manuscript.

29 April 1992; accepted 1 September 1992

Map-Based Cloning of a Gene Controlling Omega-3 Fatty Acid Desaturation in *Arabidopsis*

Vincent Arondel, Bertrand Lemieux, Inhwan Hwang, Sue Gibson, Howard M. Goodman, Chris R. Somerville*

A gene from the flowering plant *Arabidopsis thaliana* that encodes an omega-3 desaturase was cloned on the basis of the genetic map position of a mutation affecting membrane and storage lipid fatty acid composition. Yeast artificial chromosomes covering the genetic locus were identified and used to probe a seed complementary DNA library. A complementary DNA clone for the desaturase was identified and introduced into roots of both wild-type and mutant plants by Ti plasmid–mediated transformation. Transgenic tissues of both mutant and wild-type plants had significantly increased amounts of the fatty acid produced by this desaturase.

The small crucifer *Arabidopsis thaliana* (L.) is suitable for the application of map-based cloning methods because it has a small nuclear genome that is almost devoid of interspersed, highly repetitive DNA (*1*). The five chromosomes have a total DNA content of about 70,000 kb (*1*). The average distance from any gene to the nearest restriction fragment length polymorphism (RFLP) marker (*2*, *3*) is about 225 kb, and several yeast artificial chromosome (YAC) genomic libraries are available for *Arabidopsis* (*4*, *5*). Here, we used these resources to isolate a gene from *Brassica napus* that complements a mutant of *Arabidopsis* deficient in omega-3 unsaturated fatty acids.

Fatty acid desaturases catalyze the O_2 and electron donor–dependent insertion of double bonds into fatty acids. Because the amount of membrane lipid unsaturation affects the physical properties of membranes, the desaturases are thought to affect the ability of plants to survive extreme temperatures (*6*). Also, the nutritional quality of edible plant oils is largely determined by the composition of storage triacylglycerols. Except for the stearoyl-ACP desaturase, plant desaturases are thought to be membrane proteins and have been difficult to characterize by conventional biochemical methods (*7*). Information about the number and properties of the various desaturases in *Arabidopsis* has been obtained by the isolation of an extensive collection of mutants with altered membrane and storage lipid unsaturation (*8*). One of the mutations, designated *fad3*, resulted in reduced accumulation of linolenic acid ($18{:}3^{\omega 3,6,9}$), and a corresponding increase in the amount of linoleic acid ($18{:}2^{\omega 6,9}$), in extrachloroplast membrane and storage lipids (*9*). These metabolic effects suggested that the *fad3* locus encoded an ω3 linoleate desaturase.

The *fad3* locus was genetically mapped by scoring the fatty acid composition of 137 progeny (F2) of a cross between plants of the *fad3* mutant line BL1 (Landsberg race) (*9*) and wild type (Niederzenz race). Because the *fad3* phenotype is only weakly evident in chlorophyllous tissues, but is strongly expressed in root or seed tissue, the fatty acid phenotype of each F2 plant was scored by gas chromatographic analysis of the fatty acid composition of each of ten seeds obtained by self-fertilization of F2 plants. The RFLP genotype of F2 progeny was determined by analysis of DNA preparations from F2 plants and F3 families (*2*, *3*). The *fad3* mutation mapped on chromosome 2 adjacent to the RFLP markers M220 (*2*) and ASA2 (*10*) (Fig. 1). When used to screen YAC libraries, M220 hybridized with YAC EG4E8 (*4*) and ASA2 hybridized with YACs EW7D11 and EW15G1 (*5*). The YACs were ordered by analysis of hybridization of end-specific probes on Southern (DNA) blots of the YAC clones. The resultant, approximately 340 kb, contig of four YACs extended a minimum of 170 kb to the right of ASA2 (Fig. 1). As the maximum distance between M220 and ASA2 was 180 kb (the sum of the inserts in EG4E8 and EW15G1), we estimated that 1 centimorgan (cM) was equivalent to less than an average value of 105 kb in this region. As *fad3* was 0.4 cM to the right of ASA2, we estimated that the YAC contig extended far enough to the right to include *fad3*.

Stearoyl-ACP desaturase, an enzyme that catalyzes a chemically equivalent reaction, is encoded by a moderately abundant mRNA in developing seeds of oil-accumulating plants such as *Ricinus communis* (*11*). Therefore, we used the YACs to isolate moderately abundant cDNA clones. DNA from one YAC, EW7D11, was isolated from a low-melting agarose-clamped homogeneous electric field (CHEF) gel (*12*) and used to probe a λgt11 cDNA library made from developing seeds of the closely related crucifer *Brassica napus*. The *B. napus* library was used because we did not have a suitable library from developing seeds of *Arabidopsis*, and genes from *B. napus* are highly homologous to the corresponding *Arabidopsis* genes (*13*). Of 31 positive plaques among 2×10^5 screened, 17 cross-hybridized at high stringency and, therefore, appeared to be derivatives of the same gene. None of the other clones were highly represented among the 31 positive clones. The largest insert (1.4 kb) representing the abundant transcript was

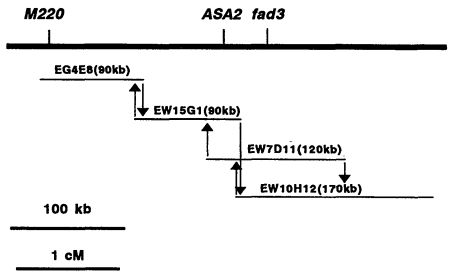

Fig. 1. Genetic map of the region of chromosome 2 (thick line) that contains the *fad3* locus. The YACs that correspond to this region of the genome are shown below. The sizes of the inserts (in parentheses), were determined by pulsed-field gel electrophoresis (*12*). Arrows indicate regions of overlap demonstrated by hybridization of end-specific probes. Scales of genetic distance (centimorgans, cM) and kilobases (kb) are indicated.

V. Arondel, S. Gibson, C. R. Somerville, MSU-DOE Plant Research Laboratory, Michigan State University, East Lansing, MI 48824–1312.
B. Lemieux, Department of Biology, York University, Toronto, Canada M3J 1P3.
I. Hwang and H. M. Goodman, Department of Genetics, Harvard Medical School, and Department of Molecular Biology, Massachusetts General Hospital, Boston, MA 02114.
*To whom correspondence should be addressed.

Table 1. Fatty acid composition of transgenic roots. The transgenic roots resulting from infection of the *fad3* mutant or wild type with *A. tumefaciens* R1000 carrying only the vector (pBI121) or the vector plus cDNA (pTiDES3) were grown in the presence of kanamycin (50 μg/ml) for 3 weeks to identify roots that had been co-transformed with one of these plasmids and 200 μg of cefotaxime to prevent growth of bacteria. The fatty acid composition of samples of roots (about 30 mg per sample) was determined as described (*23*). Abbreviations: 16:0, palmitic acid; 16:1, palmitoleic acid; 18:0, stearic acid; and 18:1, oleic acid; 18:2, linoleic acid; 18:3, linolenic acid. The values presented are the mean ± SD (n = 12).

Genotype	Fatty acid					
	16:0	16:1	18:0	18:1	18:2	18:3
	Percentage of total fatty acids					
Wild type pBI121	22.0 ± 2.9	2.5 ± 0.7	2.3 ± 1.9	3.8 ± 1.3	37.3 ± 3.7	31.9 ± 4.5
fad3 pBI121	21.2 ± 1.6	1.6 ± 0.8	2.3 ± 1.5	5.9 ± 2.6	62.2 ± 5.9	6.7 ± 0.7
fad3 pTiDES3	21.3 ± 2.3	1.5 ± 0.2	1.6 ± 0.4	9.1 ± 2.0	24.4 ± 14.9	42.1 ± 15.5
Wild type pTiDES3	21.1 ± 0.9	2.0 ± 0.1	1.9 ± 0.2	7.7 ± 2.0	15.7 ± 11.7	51.3 ± 10.9

subcloned into pBluescript (Stratagene) to produce plasmid pBNDES3.

In order to test if the cDNA in pBNDES3 was encoded by the *B. napus* equivalent of the *fad3* locus, a genetic complementation test was conducted. Because the *fad3* mutation has a large effect on the fatty acid composition of *Arabidopsis* roots (*9*), we exploited the fact that large numbers of rooty tumors can be rapidly produced by infection with *Agrobacterium tumefaciens* R1000, which carries an Ri plasmid from *Agrobacterium rhizogenes* instead of a Ti plasmid (*14*). The cDNA insert from pBNDES3 was inserted into the binary Ti vector pBI121 (Clontech Laboratories, Palo Alto, California) under transcriptional control of the constitutive cauliflower mosaic virus (CaMV) 35S promoter, to produce plasmid pTiDES3. After electroporation of pTiDES3 into *A. tumefaciens* R1000, the bacteria were used to induce rooty tumors on stem explants from the *fad3* mutant and wild-type *Arabidopsis* plants (*15*). More than 50% of the rooty tumors produced in this way contain the binary Ti plasmid and are, therefore, kanamycin-resistant (*16*). After 5 weeks, the roots were excised from the stem explants, cultured for three more weeks, and the fatty acid composition of total lipid extracts measured (Table 1). The *fad3* mutant transformed with only the vector had less 18:3 and more 18:2 fatty acid than did the wild type. Transformation of the *fad3* mutant with pTiDES3 produced roots that contained greater than wild-type amounts of 18:3 and lower amounts of 18:2. Transformation of the wild type with pTiDES3 resulted in even more 18:3. Thus, the *B. napus* cDNA in pTiDES3 functionally complements the *fad3* mutation in *Arabidopsis*, and the proportion of unsaturated lipids can be altered by affecting transcription of a putative desaturase gene.

```
        10          20          30          40
MVVAMDQRSN VNGDSGARKE EGFDPSAQPP FKIGDIRAAI
        50          60          70          80
PKHCWVKSPL RSMSYVTRDI FAVAALAMAA VYFDSWFLWP
        90         100         110         120
LYWVAQGTLF WAIFVLGHDC GHGSFSDIPL LNSVVGHILH
       130         140         150         160
SFILVPYHGW RISHRTHHQN HGHVENDESW VPLPEKLYKN
       170         180         190         200
LPHSTRMLRY TVPLPMLAYP IYLWYRSPGK EGSHFNPYSS
       210         220         230         240
LFAPSERKLI ATSTTCWSIM LATLVYLSFL VDPVTVLKVY
       250         260         270         280
GVPYIIFVMW LDAVTYLHHH GHDEKLPWYR GKEWSYLRGG
       290         300         310         320
LTTIDRDYGI FNNIHHDIGT HVIHHLFPQI PHYHLVDATR
       330         340         350         360
AAKHVLGRYY REPKTSGAIP IHLVESLVAS IKKDHYVSDT
       370         380
GDIVFYETDP DLYVYASDKS KIN
```

Fig. 2. Deduced amino acid sequence of the protein encoded by the *fad3* cDNA. The nucleotide sequence has been deposited in the GenBank database (L01418) and the clone is available from the *Arabidopsis* Biological Resource Center (*22*). Abbreviations for the amino acid residues are: A, Ala; C, Cys; D, Asp; E, Glu; F, Phe; G, Gly; H, His; I, Ile; K, Lys; L, Leu; M, Met; N, Asn; P, Pro; Q, Gln; R, Arg; S, Ser; T, Thr; V, Val; W, Trp; and Y, Tyr.

Analysis of the nucleotide sequence of the cDNA insert in pBNDES3 revealed a 383–amino acid open reading frame that encodes a 44-kD polypeptide (Fig. 2). The NH_2-terminal region does not exhibit the characteristics of a signal peptide (*17*) but the COOH-terminus contained the Lysyl residues three and five amino acids from the end that have been shown to be sufficient in animals for retention of membrane proteins in the endoplasmic reticulum (ER) membrane (*18*). Several strongly hydrophobic internal domains could be transmembrane domains. These characteristics suggest that the pBNDES3 cDNA encodes a membrane-bound protein located in the ER, which is in agreement with the available biochemical evidence concerning the localization of the ω3 desaturase encoded by the *fad3* locus (*9*). Comparison of the deduced amino acid sequence with the protein sequences contained in GenBank release 70 using the FASTA program (*19*) indicated homology with the ω6 desaturase from the cyanobacterium *Synechocystis* (*20*), including a 12-residue sequence of which 10 residues were identical. No homology with other proteins could be detected. The sequence homology between the cyanobacterial ω6 desaturase and the *fad3* gene product raises the possibility that the ω3 and ω6 desaturases in higher plants may also have significant structural similarity.

Note added in proof: J. Browse, N. Yadav, and collaborators have cloned the *Arabidopsis fad3* gene by T-DNA tagging (*21*).

REFERENCES AND NOTES

1. L. S. Leutwiler, B. Hough-Evans, E. M. Meyerowitz, *Mol. Gen. Genet.* **194**, 15 (1984); R. E. Pruitt and E. M. Meyerowitz, *J. Mol. Biol.* **187**, 169 (1986).
2. C. Chang, J. L. Bowman, A. W. DeJohn, E. S. Lander, E. M. Meyerowitz, *Proc. Natl. Acad. Sci. U.S.A.* **85**, 6856 (1988).
3. H. G. Nam, *et al.*, *Plant Cell* **1**, 699 (1989).
4. E. Grill and C. R. Somerville, *Molec. Gen. Genet.* **226**, 484 (1990).
5. E. R. Ward and G. C. Jen, *Plant Mol. Biol.* **14**, 561 (1990).
6. P. L. Steponkus, D. V. Lynch, M. Uemura, *Philos. Trans. R. Soc. London Ser. B* **326**, 571 (1990); P. Quinn, in *Plants and Temperature*, S. P. Long and F. I. Woodward, Eds. (Company of Biologists Ltd., Cambridge, 1988), pp. 237–259.
7. J. Harwood, *Annu. Rev. Plant Physiol. Plant Mol. Biol.* **39**, 101 (1988); J. Browse and C. R. Somerville, *ibid.* **42**, 467 (1991).
8. C. Somerville and J. Browse, *Science* **252**, 80 (1991).
9. B. Lemieux, M. Miquel, C. R. Somerville, J. Browse, *Theor. Appl. Genet.* **80**, 234 (1990).
10. K. K. Niyogi and G. R. Fink, *Plant Cell* **4**, 721 (1992).
11. J. Shanklin and C. R. Somerville, *Proc. Natl. Acad. Sci. U.S.A.* **88**, 2510 (1991).
12. G. Chu, D. Vollrath, R. W. Davis, *Science* **234**, 1582 (1986).
13. The six pairs of homologous genes from *Arabidopsis* and *B. napus* in GenBank release 70 had an average nucleotide sequence identity of 83%.
14. L. Moore, G. Warren, G. Strobel, *Plasmid* **2**, 617 (1979); L. D. Owens and D. E. Cress, *Plant Physiol.* **77**, 87 (1985).
15. Plants were grown for 4 weeks in continuous illumination at 23° to 25°C. Flowering stems, 10 to 20 cm in length, were surface-sterilized in 10% (v/v) Clorox, 0.02% Triton X-100, followed by four washes with sterile water. The apical 2 cm of inflorescences with flowers and unopened buds were blotted dry and the cut end dipped in an overnight L-broth culture of *A. tumefaciens*. After blotting to remove excess liquid, the stem section was pushed into the surface of agar-solidified medium so that the cut end was not in contact with the agar. The medium contained MS-salts (Gibco, Grand Island, NY), Gamborg's B5 vitamins (Gibco), 3% (w/v) sucrose, and 0.8% (w/v) agar. Following 1 day of incubation at 20° to 23°C in continuous light, the stem sections were transferred to the same medium containing cefotaxime (200 μg/ml). Hairy roots were visible at the cut ends of the sections within 15 to 20 days after infection. Individual roots were excised, and cultured on agar or as liquid cultures in 24-well dishes, in the same medium plus kanamycin (50 μg/ml).
16. J. Martinez-Zapater, J. Schiefelbein, C. R. Somerville, unpublished results.
17. G. Von Heijne, *J. Mol. Biol.* **189**, 239 (1986).
18. M. R. Jackson, T. Nilsson, P. A. Peterson, *EMBO J.* **9**, 3153 (1990).
19. W. R. Pearson and D. J. Lipman, *Proc. Natl. Acad. Sci. U.S.A.* **85**, 2444 (1988).
20. H. Wada, Z. Gombos, N. Murata, *Nature* **347**, 200 (1990).
21. J. Browse *et al.*, personal communication.

22. *Arabidopsis* Biological Resource Center, 1735 Neil Avenue, Columbus, OH 43210.
23. J. Browse, N. Warwick, C. R. Somerville, C. R. Slack, *Biochem. J.* **235**, 25 (1986).
24. We thank E. Meyerowitz for RFLP markers and mapping information, E. Ward and G. Jen for the YAC library, K. Niyogi and G. Fink for the ASA2 marker, D. Murphy for the *B. napus* library, and E. Grill, B. Hauge, J. Schiefelbein, J. Martinez-Zapater, P. Gil, and K. Iba for advice. V.A., S.G., and B.L. were supported in part by fellowships from the European Molecular Biology Organization, National Institutes of Health, and the Natural Sciences and Engineering Research Council of Canada, respectively. Supported by grants DCB8916311 from the National Science Foundation and DE-FG02-90ER20021 from the U.S. Department of Energy to C.R.S., and a grant from Hoechst AG to H.M.G.

29 June 1992; accepted 15 September 1992

Dynamics of Ribozyme Binding of Substrate Revealed by Fluorescence-Detected Stopped-Flow Methods

Philip C. Bevilacqua, Ryszard Kierzek, Kenneth A. Johnson, Douglas H. Turner*

Fluorescence-detected stopped-flow and equilibrium methods have been used to study the mechanism for binding of pyrene (pyr)-labeled RNA oligomer substrates to the ribozyme (catalytic RNA) from *Tetrahymena thermophila*. The fluorescence of these substrates increases up to 25-fold on binding to the ribozyme. Stopped-flow experiments provide evidence that pyr experiences at least three different microenvironments during the binding process. A minimal mechanism is presented in which substrate initially base pairs to ribozyme and subsequently forms tertiary contacts in an RNA folding step. All four microscopic rate constants are measured for ribozyme binding of pyrCCUCU.

Recognition of the 5′ exon for splicing of the ribosomal RNA precursor of *T. thermophila* involves base pairing of the exon sequence CUCUCU with part of an intron internal guide sequence (IGS), GGAGGG, to give a helix designated P1 (*1*). This process can be mimicked with oligonucleotides and truncated forms of the intron (*2*, *3*). Tertiary interactions involving 2′-OH groups of substrate enhance this binding (*4*–*6*). Under conditions where all the ribozyme is active (*6*), we report transient kinetic studies indicating that tertiary contacts form after base pairing, and we provide the first rate constants for the dynamics of this RNA folding step (Fig. 1A).

Conjugation of pyrene to a 5′ amino-modified ribose (Fig. 1B) provides a probe of rapid binding steps (*7*). Binding of pyrCUCU, pyrCCUCU, pyrCUCUCU, and pyrCCCUCU to the L-21 Sca I form of the ribozyme from *T. thermophila* (*3*) increases pyr fluorescence by factors of 25, 21, 8, and 4, respectively (*8*), consistent with expectations based on three-dimensional models of the binding site (*9*). All four pyr-labeled substrates reacted in single turnover nucleotidyl transfer reactions with ^{32}P-labeled (p*) p*UCGA, suggesting that their fluorescence enhancement results from binding in the catalytic core (*10*). A typical reaction modeling the second step of splicing is

pyrCCUCU	+ p*UCGA	⇌
5′exon	3′splice	L-21
mimic	junction	Sca I
	pyrCCUCUA	+ p*UCG
	5′splice	3′end
	junction	of intron

Rapid mixing, stopped-flow experiments with L-21 Sca I and pyrCCUCU resulted in fast and slow rates for binding, $1/\tau_1$ and $1/\tau_2$, respectively (Fig. 2). Traces of fluorescence versus time after mixing were fit to a single or double exponential as appropriate. Plots of rates versus [pyrCCUCU] give a straight line fit for the faster rate and a hyperbolic fit for the slower rate (Fig. 3A). This is consistent with two-step binding in which base pairing of pyrCCUCU and the IGS to form P1 occurs in the first step and uptake of P1 occurs in the second step (Fig. 1A, Scheme I). The apparent enhancement of pyr fluorescence after tertiary folding is a unique observation for a nucleic acid (*7*). For Scheme I and substrate, S, in excess over L-21 Sca I (*11*)

$$\frac{1}{\tau_1} \approx k_1[S] + k_{-1} + k_2 + k_{-2} \quad (1)$$

$$\frac{1}{\tau_2} \approx \frac{k_1[S](k_2 + k_{-2}) + k_{-1}k_{-2}}{k_1[S] + k_{-1} + k_2 + k_{-2}} \quad (2)$$

where k_1, k_{-1}, k_2, and k_{-2} are the rate constants shown in Scheme I. Initial estimates of rate constants were obtained by fitting data in Fig. 3A to Eqs. 1 and 2. Rate constants were optimized by computer simulation of traces (Table 1) (*12*). The value

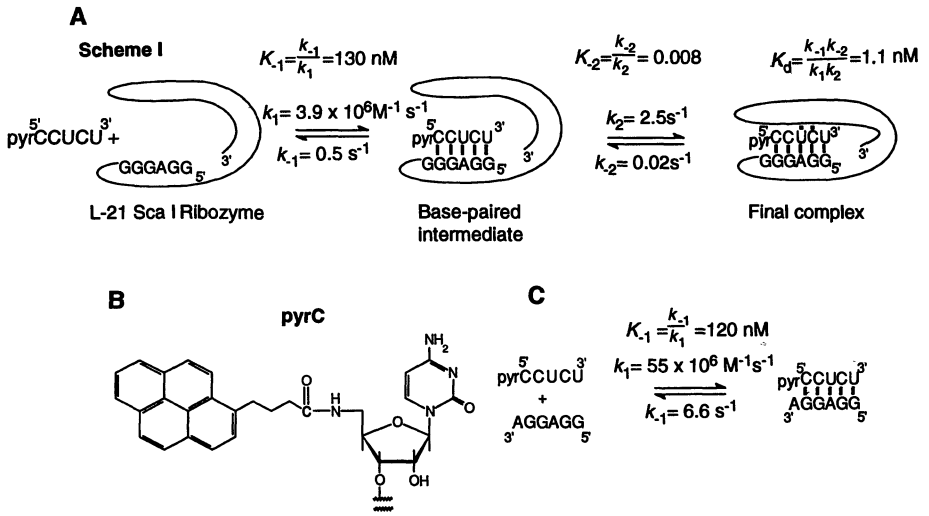

Fig. 1. (**A**) Minimal mechanism (Scheme I) consistent with all the data for all four 5′ exon mimics. The rate constants are for pyrCCUCU. The sketch of L-21 Sca I is not meant to give structural detail but to indicate that pyr is protected from solvent in both the intermediate and final state and less so as oligomer length increases. The sketch also depicts GGAGGG (IGS) as not completely accessible in the unbound L-21 Sca I. Lines indicate base pairing (*1*). Known tertiary hydrogen bonds involving 2′ OH groups of substrate (*5*, *6*) are indicated by bold dots. (**B**) Structure of the 5′ end of pyr-modified oligomers (pyrC). (**C**) Minimal mechanism for pyrCUCU and pyrCCUCU binding to the IGS mimic GGAGGA. The rate constants are for pyrCCUCU.

P. C. Bevilacqua and D. H. Turner, Department of Chemistry, University of Rochester, Rochester, NY 14627.
R. Kierzek, Institute of Bio-organic Chemistry, Polish Academy of Sciences, 60-704 Poznan, Noskowskiego 12/14, Poland.
K. A. Johnson, Department of Molecular and Cell Biology, Pennsylvania State University, Althouse Laboratory, University Park, PA 16802.
*To whom correspondence should be addressed.